

**Simulations of Arctic Mixed-Phase Clouds in Forecasts with CAM3 and AM2
for M-PACE**

*Shaocheng Xie, James Boyle, Stephen A. Klein,
Lawrence Livermore National Laboratory, Livermore, California, USA*

*Xiaohong Liu and Steven Ghan
Pacific Northwest National Laboratory
Richland, Washington, USA*

Submitted to: *Journal of Geophysical Research*

Submission Date: 07/26/2007

Manuscript No:

Revised:

Abstract

Simulations of mixed-phase clouds in forecasts with the NCAR Atmosphere Model version 3 (CAM3) and the GFDL Atmospheric Model version 2 (AM2) for the Mixed-Phase Arctic Cloud Experiment (M-PACE) are performed using analysis data from numerical weather prediction centers. The M-PACE was conducted 5 – 22 Oct. 2004 over the North Slope of Alaska and provided detailed measurements for Arctic clouds. CAM3 significantly underestimates the observed boundary layer mixed-phase cloud fraction and cannot realistically simulate the variations with temperature and cloud height of liquid water fraction due to its oversimplified cloud microphysical scheme. In contrast, AM2 reasonably reproduces the observed boundary layer cloud fraction while its clouds contain much less cloud condensate than CAM3 and the observations. The simulation of the boundary layer mixed-phase clouds and their microphysical properties is considerably improved in CAM3 when a new physically based cloud microphysical scheme is used. The new scheme also leads to an improved simulation of the surface and top of the atmosphere longwave radiative fluxes.

Sensitivity tests show that these results are not sensitive to the analysis data used for model initialization. Increasing model horizontal resolution helps capture the subgrid-scale features in Arctic frontal clouds but does not help improve the simulation of the single-layer boundary layer clouds. Changing the prescribed ice crystal number density in AM2's parameterization of the Bergeron-Findeisen process has a large impact on the simulated mixed-phase clouds and their microphysical properties, suggesting that this quantity and the Bergeron-Findeisen process need to be accurately represented in climate models.

1. Introduction

Clouds have a significant impact on the surface energy budget through modulating radiative fluxes. Observations indicate that during cold seasons, mixed-phase clouds dominate low-level Arctic clouds. The radiative properties of mixed-phase clouds are largely determined by their microphysical properties, such as cloud liquid water and ice content and number concentration. Ice generally has a much larger effective radius and therefore a much smaller optical depth for a given cloud water path compared to cloud liquid water. Thus, accurate representation of the microphysical properties of mixed-phase clouds is critical for climate models to correctly simulate cloud-radiative effects in the Arctic. Earlier studies showed that the phase partitioning between cloud liquid and cloud ice in mixed-phase clouds could have a large impact on the model predicted climate change [*Li and Le Treut 1993; Gregory and Morris 1996*].

However, the treatment of mixed-phase clouds in most current climate models is often oversimplified because the detailed microphysical processes involved in mixed-phase clouds are not completely understood due primarily to the paucity of cloud observations, which is particularly true in the Arctic. As a result, many important microphysical processes in mixed-phase clouds, such as ice nucleation and growth and the complex interaction between the ice and liquid phases of cloud condensate, are not appropriately represented in these models. For example, some climate models still use a single-moment microphysical scheme that only predicts the mixing ratio of cloud condensate. The effective radius of cloud liquid droplets is prescribed as constant. The effective radius of ice and the distinction between cloud liquid water and ice are usually assumed as a simple function of temperature. These simplified and/or empirically based microphysical parameterizations have largely limited the ability of these climate models to accurately simulate the evolution of mixed-phase clouds and their radiative properties. It is also difficult to represent aerosol-cloud coupling in these models, which requires an equation for the number concentration of cloud droplets so that the impact of aerosols on the number concentration of cloud droplets can be realistically represented. The aerosol-cloud-radiation interaction is one of the key processes that is missing in many climate models. Every major climate model is adding (if they have not done this already) this interaction.

Improving mixed-phase cloud parameterizations requires an advanced understanding of cloud and cloud microphysics through carefully planned field studies. In recent years, several

major field experiments have been conducted in the Arctic to collect the needed data for model evaluations and improvements. Examples of these field experiments include the Surface Heat Budget of the Arctic Ocean (SHEBA) project [Perovich *et al.* 1999; Uttal *et al.* 2002], the First International Satellite Cloud Climatology Project (ISCCP) Regional Experiment (FIRE) Arctic Clouds Experiment (ACE) [Curry *et al.* 2000], and the Mixed-Phase Arctic Cloud Experiment (M-PACE) [Verlinde *et al.* 2007]. Detailed in-situ observations of Arctic clouds and their microphysical properties have been obtained by using various ground based remote sensors and aircraft in these field campaigns, which provide extremely valuable information to assess and improve model cloud parameterizations.

Direct comparison between climate model simulations and field experiment observations is difficult because climate simulations represent statistics of the atmospheric evolution and are not initialized to any specific time observed during the field campaigns. In order to make a direct model-observation comparison, this study makes use of a tool developed from the Department of Energy (DOE) CCPP-ARM Parameterization Testbed (CAPT) project to initialize climate models with analysis data from Numerical Weather Prediction (NWP) center's data assimilation systems and then evaluate climate models in their short-range weather forecasts using field measurements. Here CCPP and ARM are the DOE Climate Change Prediction Program and Atmospheric Radiation Measurement Program, respectively. The CAPT approach has been proven as a useful way to understand climate model errors and facilitate model parameterization improvements [Phillips *et al.* 2004; Xie *et al.* 2004; Boyle *et al.* 2005, Williamson *et al.* 2005; Sud *et al.* 2006; Klein *et al.* 2006]. By initializing climate models with realistic atmospheric states from NWP analyses for the period where a selected field campaign was conducted under the CAPT framework, the detailed evolution of parameterized variables in short-range weather forecasts can be compared with field experiment data and model deficiencies can be linked directly with specific atmospheric processes observed during the field campaign. Running climate models in NWP mode also allow us to identify specific parameterization deficiencies before the compensation of multiple errors masks the deficiencies, as can occur in model climate simulations.

In this study, two major U.S. climate models, the National Center for Atmospheric Research (NCAR) Community Atmospheric Model version 3 (CAM3) NCAR CAM3 and the NOAA Geophysical Fluid Dynamics Laboratory (GFDL) climate model (AM2), are tested under

the CAPT framework against the data collected from the ARM M-PACE field campaign. M-PACE was conducted during the period from 5 – 22 October 2004 near the ARM North Slope of Alaska site and provided a complete set of measurements for Arctic clouds and their microphysical properties by using millimeter-wave cloud radars (MMCR), micropulse lidars, laser ceilometers, and aircraft [Verlinde *et al.*, 2007]. This study attempts to identify potential deficiencies related to the cloud and cloud microphysical schemes used in these two climate models by a direct comparison of model results with the in-situ and remote sensing data from M-PACE. A new physically based cloud microphysical scheme is also tested in CAM3 to help understand how cloud microphysical processes affect the evolution and phase partitioning of the mixed-phase clouds. The sensitivity of the model results to initial data, model resolution, and ice crystal number concentration is discussed.

The manuscript is organized as follows. Section 2 briefly describes the models and model initialization procedure, with some details given on their cloud and cloud microphysical schemes. A new ice microphysical scheme for CAM3 is also described in this section. Section 3 compares model results with the M-PACE observations. Section 4 shows results from the sensitivity tests. A summary of this study is given in section 5.

2. Models and Model initialization

2.1. CAM3

CAM3 is the NCAR atmospheric general circulation model (GCM) version 3. CAM3.1 with its finite volume dynamic core at resolution of $1.9^{\circ} \times 2.5^{\circ}$ in the horizontal and 26 levels in the vertical is used in this study. Compared to its earlier versions, CAM3 incorporates significant improvements to its physical parameterizations of clouds and radiation. The treatment of cloud microphysics and cloud condensate in CAM3 is based on the prognostic cloud water formulation of *Rasch and Kristjansson* [1998, hereafter RK98] with modifications made by *Zhang et al.* [2003]. RK98 is a single-moment scheme that only predicts the mixing ratio of cloud condensate. The distinction between liquid and ice phase is made as a function of temperature. The fraction of liquid water in the total condensate is defined as:

$$\begin{aligned}
 f_l &= 0 && \text{if } T \leq T_{\min} \\
 f_l &= (T - T_{\min}) / (T_{\max} - T_{\min}) && \text{if } T_{\min} < T < T_{\max} \quad (1)
 \end{aligned}$$

$$f_i = 1 \quad \text{if } T \geq T_{\max}$$

where T is temperature, $T_{\min} = -40^{\circ}\text{C}$, and $T_{\max} = -10^{\circ}\text{C}$. Further improvements beyond RK98 include separate equations for predicting cloud ice and cloud liquid water, advection of cloud condensate by large-scale circulation, and gravitational settling of cloud ice and liquid particles [Boville *et al.* 2006]. However, Eq. (1) is still applied each time step to repartition the cloud liquid water and cloud ice. Cloud fraction in CAM3 is diagnosed for convective clouds based on convective mass flux and for stratiform clouds (C_s) based on relative humidity (RH) outside of the convective cloud according to

$$C_s = ((\text{RH} - \text{RH}_{\min}) / (1 - \text{RH}_{\min}))^2 \quad (2)$$

RH is calculated with respect to water (RH_w) for $T > 0^{\circ}\text{C}$ and with respect to ice (RH_i) for $T < -20^{\circ}\text{C}$ and is interpolated using RH_w and RH_i between -20°C and 0°C . The threshold relative humidity RH_{\min} varies with pressure. Other detailed information about CAM3 can be seen in Collins *et al.* [2006].

A physically based ice microphysical scheme described in Liu *et al.* [2007] (LIU07) with slight modifications is also tested in CAM3 to help understand how cloud microphysical processes affect the cloud evolution and ice crystal growth in the mixed-phase clouds. LIU07 is a double-moment scheme in which a prognostic equation is used for ice crystal number concentration together with an ice nucleation scheme developed by Liu and Penner [2005]. The liquid and ice mixing ratio is still calculated by the modified RK98 scheme described in Boville *et al.* [2006] but the liquid mass conversion to ice due to the deposition growth of ice crystals at the expense of liquid water (Bergeron-Findeisen process) is based on the Rotstayn *et al.* [2000] scheme. The original Rotstayn *et al.* [2000] scheme assumes a direct conversion from liquid to ice to maintain liquid water saturation inside in mixed-phase clouds while LIU07 assumes a conversion from water vapor to ice, which results in a smaller conversion rate of liquid to ice in mixed-phase clouds. In this study, we slightly modify LIU07 to allow a direct conversion from liquid to ice as it was assumed in the original Rotstayn *et al.* [2000] scheme but assume saturation that is weighted by the proportions of ice and liquid water mass for mixed-phase clouds. Another important change to CAM3 by using LIU07 is that the effective radius of ice

crystals is now based on the predicted mass and number concentration of ice rather than diagnosed as a function of temperature as in the default model. This will make the computation of model radiation more sensitive to cloud properties. The stratiform cloud fraction is calculated using the same RH-based scheme as that in the default model except that ice super-saturation is allowed in the upper troposphere in the new scheme. As shown later, this can have an impact on simulated cloud fraction.

2.2. AM2

AM2 is the GFDL climate atmospheric model. The model resolution used in this study is $2.0^{\circ} \times 2.5^{\circ}$ in horizontal and 24 levels in vertical. Its cloud microphysical scheme follows Rotstayn [1997] and Rotstayn et al. [2000], in which two separate prognostic equations are used to predict cloud liquid and ice and the liquid/ice partitioning is determined by microphysical processes including the Bergeron-Findeisen mechanism. This microphysical scheme is a single-moment scheme. Cloud fraction in AM2 is determined by a prognostic cloud fraction scheme developed by *Tiedtke* [1993]. Further details are available from *GFDL GAMDT* [2004].

It is noted that both LIU07 and AM2 use the *Rotstayn et al.* [2000] scheme for liquid water conversion to ice (Bergeron process) in the mixed-phase clouds. Similar to *Rotstayn et al.* [2000], AM2 assumes that the growth of ice crystals is at the expense of the evaporation of cloud liquid to maintain the liquid water saturation in clouds. This could result in a slightly faster conversion rate of liquid to ice in AM2 than that in the slightly modified LIU07 tested in this study since the saturation vapor pressure with respect to ice is lower than that with respect to liquid. Another major difference between LIU07 and AM2 is the treatment of ice crystal number. LIU07 uses a prognostic equation to predict the ice crystal number by considering the processes of advection, convective transport, ice nucleation, droplet freezing, microphysical conversion to precipitation, and cloud evaporation. The ice nucleation mechanisms in LIU07 include the homogeneous ice nucleation on sulfate aerosol and heterogeneous immersion nucleation on soot particles in cold clouds with temperature less than -35°C [*Liu and Penner, 2005*]. In mixed-phase clouds with temperatures between -40° and -3°C , contact freezing of cloud droplets through the Brownian coagulation with insoluble ice nucleation is considered. Contact ice nuclei are assumed to be mineral dust [*Lohmann, 2002*]. Deposition/condensation ice nucleation is parameterized assuming the *Meyers et al.* [1992] (see Eq. (3) in Section 4) function of ice

supersaturation. Secondary ice production between -3 and -8 °C is based on *Cotton et al.* [1986] for Hallet-Mossop multiplication. In contrast, the ice crystal number in AM2 is simply determined by the *Meyers et al.* [1992] parameterization. Additional discussion on this will be given in Section 4. Other differences between LIU07 and AM2 include that the former allows ice supersaturation while the latter does not.

2.3. Model initialization

Both CAM3 and AM2 were initialized from the NASA Data Assimilation Office (DAO) analysis data for M-PACE. More information about the DAO analyses is available at <http://gmao.gsfc.nasa.gov/>. The analysis data were interpolated from the finer-resolution reanalysis grid ($0.5^{\circ} \times 0.5^{\circ}$) to the CAM3 or AM2 grid using the procedures described in *Boyle et al.* [2005]. These procedures used a slightly different interpolation approach for each of the dynamic state variables, i.e., horizontal winds, temperature, specific humidity and surface pressure, along with careful adjustments to account for the difference in representation of the earth's topography between models. It was judged by comparing with the sounding data collected during the experiment that the DAO analyses reasonably captured the temporal evolution and vertical structure of the observed upper-air circulation, temperature, and moisture during M-PACE. This is important since the observed cloud systems during M-PACE are largely controlled by the synoptic-scale circulation [*Verlinde et al.* 2007].

A series of 3-day forecasts with CAM3 and AM2 are initialized every day at 00Z from the DAO analyses for the entire period of M-PACE from 5 – 22 October 2004. The data from the 12-36 hour forecasts are examined in order to reduce the impact of model spin-up that may occur in the first few hours of an integration. In this forecast range, the atmospheric state is still close to the observation so that model errors can be primarily linked to deficiencies in model physics. Results at the model grid point that is closest to the ARM Barrow site (156.4W, 71.33N) are compared with the M-PACE observations. The location of the selected model grid point is (155W, 72N) for CAM3 and (156.25W, 71N) for AM2. We have examined model results at other nearby grid points and seen some spatial variations in the simulated clouds, but the spatial variations in the simulated clouds among these nearby grid points are much smaller than the differences between model simulations and the observations as shown in next section.

3. Results

3.1 Characteristics of clouds observed from M-PACE

Various types of clouds that often occur in the Arctic during its transition season were observed in the M-PACE field experiment. Figure 1a shows the time-pressure cross section of observed cloud fraction at Barrow by integrating measurements from the ARM cloud radar and other sensors using the ARSCL (Active Remotely-Sensed Clouds Locations) algorithm [Clothiaux *et al.* 2000]. It is seen that Barrow was covered with multilayered stratus clouds in the mid- and low-levels with the cloud top up to 550 hPa for 5 – 8 October, persistent single-layer boundary layer stratocumulus with the cloud top around 850 hPa during the period from 8 to 14 October, and deep prefrontal and frontal clouds (including cirrus) from 15 – 22 October.

The observed cloud systems were largely controlled by the synoptic-scale circulation affecting that area during M-PACE. As described in Verlinde *et al.* [2007], for the period from 5 – 15 October, the NSA was dominated by a strong surface high-pressure system built over the pack ice to the northeast of the Alaska coast. Associated with the strong surface high, east-northeasterly flow prevailed at low levels. The low-level northeasterly flow combined with a midlevel low pressure system drifted along the northern Alaska coast generated the complicated multilayer cloud structure over NSA from 5 – 7 October. The single-layer low-level clouds observed from 8 – 15 October originally formed over the ocean adjacent to the Alaskan coast as the low-level east-northeasterly flow brought cold near-surface air from the pack ice to the warm ocean and then advected to Barrow. During this period, there was a substantial temperature decrease at altitudes below the 665 hPa pressure level and a sharp moisture decrease over the Barrow site. The range of cloud temperature was from -5°C to -20°C , indicating that the cloud condensate was mixed phase. After 14 October, the boundary layer clouds started to disappear as a warm front moved through the area on 15-16 October and a deep ridge moved over the NSA. Southwesterly flow prevailed in the entire troposphere except on late 19 October when there was an abrupt wind direction change from the southwest to the southeast associated with a strong warm frontal passage which brought in deep prefrontal and frontal clouds. Cirrus clouds were seen during this period.

To obtain in-situ and remote sensing measurements of microphysical properties of these cloud systems, the ARM millimeter cloud radar, micropulse lidars, laser ceilometers, and two instrumented aircraft were used in the experiment. For the single-layer boundary layer clouds,

data collected from both the surface-based remote sensing instruments and the aircraft revealed the presence of a maximum liquid water layer near cloud top and liquid and irregular ice crystals within the cloud layer with precipitating ice beneath the liquid cloud base [McFarquhar *et al.* 2007]. This result is consistent with the findings from other arctic field campaigns [Pinto 1998; Hobbs and Rangno 1998; Curry *et al.* 2000]. The multilayered clouds had a more complicated structure than the single-layer clouds. Up to six liquid cloud layers were detected by the ARM narrow-band lidar and the depth of individual liquid cloud layers varied from 50 to 300 m. Combined radar and lidar data indicated the existence of precipitating ice with low ice crystal concentration between the layers. These characteristics are similar to those from the in situ measurements by the aircraft. A detailed summary of the observed clouds during M-PACE can be seen in Verlinde *et al.* [2007] and McFarquhar *et al.* [2007]. In the following discussion, we examine how well CAM3 and AM2 capture these observed features in the arctic clouds.

3.2 Model-simulated clouds

Figures 1b, 1c, and 1d show the model-produced cloud fraction at Barrow from CAM3, AM2, and the CAM3 with the new ice microphysics described in section 2 (hereafter CAM3LIU), respectively. All the models are able to qualitatively reproduce the cloud types observed during M-PACE, such as the multilayered clouds from 5 – 8 October, the boundary layer clouds from 8 – 14 October, and the frontal deep high clouds from 15 – 22 October. However, there are considerable differences in detailed structures of the clouds between the observations and the model simulations. For the period 5 – 14 October, the default CAM3 substantially underestimates the observed multi-layered and single-layer boundary layer cloud fraction. In contrast, AM2 produces much more mid- and low-level cloud fraction than CAM3. It is interesting to see that the CAM3 with the new ice microphysics produces more realistic single-layer boundary clouds than the default CAM3 while it generates too many mid- and high level clouds. The overestimation of mid- and high level clouds is partially related to the scheme's allowance of ice supersaturation. As discussed earlier, CAM3 uses a RH-based cloud scheme to diagnose stratiform cloud fraction (Eq. (2)). Given the same threshold RH_{\min} , the new scheme would lead to more cloud fraction than the default CAM3 due to the allowance of ice supersaturation. We have found that the RH in CAM3LIU is often supersaturated with respect to ice in the mid- and high levels where temperature is usually less than -20°C during M-PACE.

One common problem for all the models is that the modeled cloud top and cloud base are lower than the observed for the period 8 – 15 October. The averaged cloud [top, base] pressures over this period for ARSCL, CAM3, CAM3LIU, and AM2 are [840, 939], [855, 985], [851, 991], and [865, 1006] (hPa), respectively. This may be partially related to the coarse vertical resolutions used in these models, which cannot well resolve the observed boundary layer structure. For example, CAM3 only has four model levels below 850 hPa, the level of the observed single-layer boundary layer cloud top. Note that the cloud base in the ARSCL products is determined by the ARM laser ceilometers and micropulse lidars, which are usually insensitive to ice precipitation (if the concentration of precipitation particles is not sufficiently large) or clutter and can provide quite accurate cloud base measurements [*Clothiaux et al.*, 2000]. For the deep frontal clouds, the models tend to overestimate the clouds at high levels and underestimate them at mid- and low levels. The problem with the mid- and low-level clouds is particularly severe for the CAM models. In addition, the model-simulated frontal clouds tend to have a longer lifetime and weaker temporal variability than the observed. This is a common problem for most large-scale models in simulating frontal clouds [e.g., *Klein and Jakob*, 1999; *Zhang et al.*, 2005; *Xie et al.* 2005]. The temporal variability in the observed frontal clouds is partially related to subgrid-scale dynamics which cannot be resolved in large-scale models. The difference in temporal variability between the models and observations may also due to the fact that the ARM observations are from a point whereas the models are grid box averaged.

Figure 2 compares the total cloud fraction between the models and the observations at Barrow. The observed total cloud fraction is calculated from the ARSCL products assuming maximum cloud overlap. The observations typically showed a persistent almost 100% cloud cover during the period 5 – 14 October except on 7 – 8 and 11 October where the cloud cover decreased slightly. Consistent with earlier discussions, CAM3 considerably underestimates the total cloud cover for this period. This problem is significantly reduced in CAM3LIU when the new physically based ice microphysical scheme is used. AM2 also produces a much better cloud cover than the default CAM3. It is seen that the cloud fraction produced by the default CAM3 shows larger temporal variability than the observations, indicating the difficulty in maintaining the persistence of mixed-phase boundary layer clouds in this model. In contrast, CAM3LIU and AM2 have 100% cloud cover for most of the period 5 – 14 October, similar to the observations. The model ability to maintain the long life of mixed-phase boundary layer clouds will have large

impacts on the surface radiation in the Arctic as discussed later. For the deep frontal clouds, both CAM3LIU and AM2 largely overestimate the observed cloud fraction while CAM3 generally agrees well with the observation.

Figures 3a-c show the grid box mean liquid water mixing ratio (LWC) produced from these models. The contour lines in Figure 3 are the model produced temperatures. All the models are able to produce two or more liquid cloud layers for the period 5 – 8 October even though the fine vertical structures of the observed multi-layer clouds as shown in *Verlinde et al.* [2007] are not well simulated due to the coarse model vertical resolution. In comparison with CAM3LIU, CAM3 predicts similar amount of cloud liquid water for the boundary clouds even though its cloud fraction is much lower. This is partially due to its temperature dependent liquid/ice partitioning. For the range of temperature $-5^{\circ}\text{C} \sim -20^{\circ}\text{C}$, the majority of cloud condensate produced in CAM3 will be liquid. Another noteworthy feature is that CAM3 has much more liquid in the mid- and upper level clouds than both CAM3LIU and AM2, which leads to a considerable overestimation of the observed liquid water path in CAM3 during these periods. It is noted that AM2-produced clouds contain much less liquid than CAM3LIU for the mixed-phase boundary clouds although they produce comparable cloud fraction and include the Bergeron-Findeisen microphysical process. This suggests a faster conversion rate of liquid to ice in AM2 than CAM3LIU, which should be partially related to the differences in specifying the vapor saturation and the ice crystal number concentration between these two models as discussed in Section 2.2.

Figure 4 is the same as Figure 3 except for ice water mixing ratio. Since there is no distinction between ice and snow inside the cloud for AM2 (i.e., AM2 ice includes snow inside the cloud) but for CAM3 there is, we add model snow field to the ice water mixing ratio in CAM3 and CAM3LIU for a better comparison with AM2. For simplicity, we use “ice” to represent the sum of ice and snow in our following discussions. It should be noted that the snow in CAM3 and CAM3LIU has no impact on radiation while the snow inside cloud in AM2 affects model radiation since it is treated as ice. Compared to CAM3 and CAM3LIU, AM2 produces less ice for boundary layer clouds and near the surface partially due to the fact that the snow falling out of clouds is not included in Figure 4b while it produces significantly larger ice in the strong frontal clouds on 19 October. Generally, CAM3LIU generates more ice than the default CAM3, especially for the boundary layer mixed-phase clouds.

Figures 5a and 5b show the observed and modeled cloud liquid water path (LWP) and cloud ice water path (IWP) at Barrow, respectively. Note that both observed and modeled IWPs include snow component since the observations cannot separate snow from ice. There are two sources for the observed LWP. Both are based on the ARM surface Microwave Radiometer (MWR) measurements but they are retrieved using different retrieval algorithms. One is based on the algorithm described in *Turner et al.* [2007] and another one is derived using *Wang* [2007]. The observed IWP is derived from the ARM cloud radar and lidar measurements [*Wang*, 2007]. The remote sensing retrieved IWP is currently available for the single-layer boundary layer mixed-phase clouds. The instrument uncertainty is typically within 5% for LWP and 50% for IWP. It is seen that the LWPs from these two measurements agree with each other very well for the period when the radar and lidar retrievals are available. CAM3 reasonably reproduces the observed LWP for the single-layer mixed phase clouds even though its cloud amount is significantly smaller than the observations. This inconsistency between LWP and cloud fraction in CAM3 is due to the fact that CAM3 cloud fraction is determined by its large-scale relative humidity rather than its cloud condensate. One clear problem with the default CAM3 is that it largely overestimates the observed LWP for the mid- and high level clouds (e.g., Oct. 7, 16, 18 – 20). This problem is significantly reduced with the use of the new ice microphysical scheme as shown in CAM3LIU, which also predicts a reasonable LWP for the boundary layer clouds. Consistent with earlier discussion, the LWP in AM2 is considerably smaller than the CAM models and the observations for the boundary layer clouds, suggesting the conversion rate of liquid to ice might be too fast in AM2. However, it is surprising to see that the single-layer boundary layer clouds produced by AM2 do not have much ice either. One possible explanation is that cloud condensate in AM2 grows much faster to precipitable size and falls out of the model atmosphere compared to the CAM models. This is evident from the fact that AM2 generates larger surface precipitation rates than the CAM models during this period. The average surface precipitation rates over the period from Oct. 9 – 14 are 0.7 mm/day for AM2, 0.43 mm/day for CAM3, and 0.42 for CAM3LIU. For the frontal clouds occurred 15 – 22 October, the IWPs simulated by CAM3 and CAM3LIU agree with each very well while AM2 produces significantly large IWP than CAM3 for the strong deep frontal clouds on 19 October, which again suggests more rapid glaciations occurred in AM2 than the CAM models for this case.

3.3 Microphysical properties in the single-layer mixed-phase clouds: model vs. aircraft data

The instrumented aircraft used in M-PACE provided unique information to understand the microphysical properties in the mixed-phase clouds. Figure 6a displays the liquid fraction (f_l) in the total cloud condensate as a function of height measured by the University of North Dakota (UND) Citation from flights on 9 – 10 October for the single-layer mixed-phase clouds. Note that the aircraft measured total cloud condensate contains snow. The raw aircraft data were at 10 second time interval and processed by *McFarquhar et al.* [2007]. The cloud altitude is normalized from 0 at liquid cloud base to 1 at cloud top. The different color dots in Figure 6a represent data collected from different flights. The aircraft data revealed the dominance of cloud liquid water in the boundary layer mixed-phase clouds with 79% of cases having $f_l > 90\%$. In general, f_l increases with height and is larger than 80% near cloud top. Many data points with low f_l are found in the lower half of the cloud, indicating the presence of significant amounts of ice. The strong liquid layer near cloud top leads to strong cloud-top radiative cooling, which may play an important role in maintaining the persistence of mixed-phase boundary layer clouds [e.g., *Pinto, 1998*].

Figures 6b-6d is the same as Figure 6a except for CAM3, AM2, and CAM3LIU, respectively. The snow component is added to the total cloud condensate when the modeled liquid fraction is calculated in order to be consistent with the aircraft measurements. This observed vertical distribution of f_l is clearly not reproduced by CAM3 in which f_l generally decreases with height due to its temperature dependence. The few points with low f_l found at the cloud base in Figure 6b are due to the model-produced snow. In contrast, the observed variation of liquid water fraction with cloud height is reasonably captured by CAM3LIU. AM2 also shows a better agreement with the observations than CAM3. The lack of low f_l points near the cloud base in AM2 is probably due to the fact that the snow falling out of the cloud is not included in the AM2 total cloud condensate when f_l is calculated.

Figure 7a shows the measured f_l as a function of temperature from the same flights as Figure 6a. The measured cloud temperatures during these flights are about between -16°C to -9°C . It is seen that there is no clear relationship between f_l and temperature in the observations. Significant amounts of liquid and ice co-exist within this temperature range. It is obvious that any temperature based liquid/ice partitioning schemes will fail to reproduce the observed structure, such as the scheme used in CAM3 (see Figure 7b). Once again, AM2 and CAM3LIU

reasonably reproduce the observed variation with temperature of f_1 by including the Bergeron-Findeisen process (Figures 7c-d). This indicates that the Bergeron-Findeisen process is critical for the models to correctly capture observed structure of cloud condensate in the mixed-phase clouds.

3.4 Radiation

Clouds have a large impact on surface radiation. However, it is difficult to evaluate model shortwave radiation (SW) with point measurements taken at a station located near the coast (e.g., Barrow). The closest CAM and AM2 model output grid points to the Barrow site cover both ocean and land areas, over which the surface characteristics are very different. For example, there is a very strong contrast in the surface albedo between ocean and land. During M-PACE, the ARM Barrow site was covered by snow with the surface albedo in a range of 0.7 to 0.9 [Xie *et al.* 2006] while its nearby ocean was open water, which had much smaller surface albedo (less than 0.2). The difference in the surface albedo between the models and the observations makes it difficult to interpret model-observation comparison since surface albedo has a large impact on both the surface upward and downward radiation, in addition to clouds. Thus, in this study we will focus our discussion on the surface downward longwave radiation and the top of the atmosphere (TOA) outgoing longwave radiation, which are more related to clouds and less dependent on surface conditions. Moreover, longwave radiative fluxes are the dominated terms in the surface and TOA energy budgets in the cold Arctic season.

Figure 8a displays the observed and modeled downward longwave radiative fluxes (LW) at surface. The observed surface radiation data are obtained from the ARM Solar and Infrared Radiation Station. For the period 5 – 14 October, the observed surface downward LW shows a rather weak temporal variability due to the presence of persistent low-level clouds. The observed value is significantly underestimated by CAM3, due primarily to its underestimation of the low-level clouds as shown in Figures 1 and 2. In addition, CAM3 shows much larger temporal variation in the surface downward LW than the observations, consistent with the larger temporal variation in its produced cloud cover (Figure 2). These problems are largely reduced in CAM3LIU, which only slightly overestimates the observations for the period 10 -14 October. The overestimation may be related to the lower cloud base altitude in CAM3LIU. AM2 also shows a better simulation of the surface downward LW than CAM3. Its produced surface

downward LW agrees well with the observations for most of the period while it significantly underestimates the observations on Days 9, 13, and 14 associated with the problem with its simulated cloud field. The averaged surface downward LWs over the period 5 – 14 October are 284, 264, 291, and 278 (W/m²) for the observations, CAM3, CAM3LIU, and AM2, respectively. For the period 15 – 22 October, all the models generally overestimate the observed surface downward LW, partially due to the longer lifetime for the frontal clouds simulated by these models.

Figure 8b is the same as Figure 8a except for the outgoing longwave radiative fluxes (OLR) at top of the atmosphere. The observed TOA radiative fluxes are from the 1° x 1° analysis of the NASA Terra and NOAA 16 satellite measurements. All the models consistently overestimate the observed OLR in the presence of the single-layer boundary layer clouds (9 -14 October). This is related to the underestimation of the cloud fraction and cloud liquid water path during this period as discussed earlier. The model underestimation of the low-level cloud top altitude may also contribute to this problem. Compared to CAM3, the overestimation is largely reduced in CAM3LIU. It is seen that CAM3LIU considerably underestimate the observed OLR on day 7 when the multi-layered clouds occurred. This is mainly because CAM3LIU clouds extend to much higher altitude (300 hPa) than the observed (~ 550 hPa) (see Figure 1). For the deep frontal period, the smaller OLR produced by the models on 15-16 October and 17-18 October is consistent with the higher frontal cloud fraction generated by these models compared to the observations.

4. Sensitivity tests

Several sensitivity tests are conducted to illustrate how sensitive model results are to initial data, model resolution, and ice crystal number concentration. As mentioned earlier, the CAPT approach is to initialize a climate model with the NWP analyses without developing its own data assimilation system. Since the NWP analyses are not perfect and are affected by deficiencies in the model used to produce the analysis, model results may be sensitive to the analyses from different NWP centers. Thus, it is useful to examine if the model behaviors shown in this study are robust and not dependent on a particular analysis. For this purpose, we tested CAM3 and CAM3LIU with the National Center for Environmental Prediction (NCEP) Global Data Assimilation System (GDAS) analysis data (<http://wwwt.emc.ncep.noaa.gov/gmb/gdas/>)

for M-PACE. Similar to the DAO analyses, the GDAS analyses also reasonably represent the observed atmosphere for M-PACE but with slightly smaller biases of generally less than 1 K in temperature and 0.1 g/kg in moisture compared to the errors of less than 1.5 K in temperature and 0.1 g/kg in moisture in the DAO analyses. We found that the forecasts of clouds and cloud microphysical properties with the GDAS data are very similar to those with the DAO analyses as shown in Section 3. This indicates that the errors associated with the simulated mixed-phase clouds in CAM3 and the improvements seen in CAM3LIU with the new ice microphysical scheme are rather robust with respect to conditions with initial data.

Another two sensitivity tests were conducted with AM2: AM2N90 is AM2 with a higher horizontal resolution of $1.0^{\circ} \times 1.25^{\circ}$ and AM2N90N is the same as AM2N90 but with a modified parameterization of ice crystal number density based on the M-PACE observations. As described in Section 2.2, AM2 uses a parameterization of the Bergeron process based upon *Rotstayn et al.* [2000]. The parameterization is based upon the diffusional growth of ice crystals in the presence of liquid drops that maintain the ambient water vapor at liquid water saturation (and thus ice-supersaturation). The Bergeron process is proportional to the assumed number density of crystals to the $2/3$ power. Since AM2 does not have a prognostic equation for the number density of crystals, this is parameterized following *Meyers et al.* [1992]:

$$N_i = \exp[12.96(e_{sl} - e_{si})/e_{si} - 0.639] \quad (3)$$

Where N_i (L^{-1}) is the ice crystal number concentration, e_{sl} is the saturation vapor pressure of liquid, and e_{si} is the ice saturation vapor pressure. The constant parameters used in Eq. (3) are empirically determined from mid-latitude measurement of ice nuclei (IN) concentrations for the temperature range from $-7^{\circ}C$ to $-20^{\circ}C$, which are generally much higher than Arctic IN concentrations [e.g., *Bigg*, 1996]. In order to best fit M-PACE observations of ice nuclei, *Prenni et al.* [2007] modified Eq. (3) to

$$N_i = \exp[1.87(e_{sl} - e_{si})/e_{si} - 1.488] \quad (4)$$

In the sensitivity study (AM2N90N), Eq. (4) is used to calculate the ice crystal number density used in the parameterization of the Bergeron process. At the typical temperature range of

M-PACE clouds (-10°C to -15°C), Eq. (4) results in a much smaller ice crystal number density of 0.29 L^{-1} as compared to 3.23 L^{-1} from Eq. (3).

It should be noted that the ice nuclei (IN) concentrations used to obtain Eq. (4) were obtained from the measurements of a Continuous Flow Diffusion Chamber (CFDC) aboard the Citation aircraft used in M-PACE. The CFDC is sensitive to all nucleation modes, except contact freezing. The CFDC measurements represent the total number concentration of active IN that have diameters less than $2\text{ }\mu\text{m}$ acting in deposition, condensation, and immersion-freezing models. The CFDC IN concentrations are often dramatically different from the ice crystal number concentration measured by the cloud probes (e.g., one- or two-dimensional cloud probes and the Forward Scattering Spectrometer Probe) partly due to differences in CFDC processing conditions and ambient conditions [Prenni *et al.*, 2007]. For the flights taken on 9 – 10 October for the single-layer mixed phase clouds, the CFDC measured IN varies from 0.1 to 1 L^{-1} , which is considerably lower than the ice crystal number concentration measured by the cloud probes, which generally varies from 0.1 to 10 L^{-1} with an average of 2.8 L^{-1} and a standard deviation of 6.9 L^{-1} [McFarquhar *et al.*, 2007]. It is noted that the averaged ice crystal number concentration predicted by CAM3LIU over these flight periods is around 2.74 L^{-1} , which agrees well with the cloud probe measured values. It is also noteworthy that the ice crystal number concentrations in the AM2 standard run are slightly higher than those predicted in CAM3LIU, which is one of the reasons that AM2 has faster conversion rate of liquid to ice than CAM3LIU as discussed earlier.

Figure 9a displays the simulated clouds from AM2N90 at the model grid point (155.625W , 71.5N) closest to Barrow for M-PACE. Compared to the default AM2, AM2N90 produces slightly smaller cloud fraction for the multilayered and single-layer boundary layer clouds. The mid-level clouds from Oct. 5-8 are not well captured by AM2N90. As one can expect that the observed temporal variability in deep frontal clouds from Oct. 15-22 is better reproduced in AM2N90 since the frontal scale circulations are better resolved with increasing the model horizontal resolution. It is seen that AM2N90-produced clouds contain slightly more liquid water than AM2-simulated, but they are still less than the observations (Figure 10a). The IWP produced by AM2N90 is very similar to that in AM2 (Figure 10b).

The AM2 simulated clouds and cloud properties are very sensitive to the change in the parameterization of ice crystal number concentration. In general, the smaller ice crystal number density used in AM2N90N leads to a significant increase in both cloud fraction (Figure 9b) and

cloud liquid water path for the period Oct. 6 -15 (Figure 10a) while there is only a small change in the simulated cloud ice in comparison with AM2N90 (Figure 10b). It is noteworthy that the AM2N90N simulated multi-level and boundary layer clouds are higher in altitude and more close to the observations than AM2N90. These results illustrate the importance of accurately representing detailed cloud microphysical properties in climate models. It should be noted that there are still rather large discrepancies in the LWP between AM2N90N and the observations, indicating that other model deficiencies also contribute to the errors in the AM2 simulated mixed-phase clouds.

5. Discussion and summary

We have evaluated the mixed-phase cloud parameterizations used in the two major U.S. climate models, the NCAR CAM3 and GFDL AM2, in short-range forecasts under the DOE CCPP-ARM Parameterization Testbed (CAPT) against the in-situ and remote sensing data collected from the ARM M-PACE field experiment over NSA. We have shown that both models are able to qualitatively capture the various cloud types observed during the M-PACE when they are initialized with realistic atmospheric conditions from the DAO analyses. However, there are significant differences in the simulated cloud fraction and cloud microphysical properties between the two models and between the models and the observations. CAM3 significantly underestimates the observed boundary layer cloud fraction and cannot realistically simulate the variations with temperature and cloud height of liquid water fraction in the total cloud condensate due to an oversimplified cloud microphysical scheme. It also largely overestimates the liquid water path for mid- and high level clouds. AM2 reasonably reproduces the observed boundary layer cloud fraction while its clouds contain much less cloud condensate than CAM3 and the observations. The simulation of the boundary layer mixed-phase clouds and their microphysical properties is considerably improved in CAM3 when a more physically based cloud microphysical scheme is used. The new scheme also leads to an improved simulation of the surface and top of the atmosphere longwave radiative fluxes. This study has shown that the Bergeron-Findeisen process, i.e., the ice crystal growth by vapor deposition at the expense of coexisting liquid water, is important for the models to correctly simulate the characteristics of the observed microphysical properties in mixed-phase clouds.

Sensitivity tests have shown that these results are not sensitive to the initial data produced

from two different NWP centers. Increasing model horizontal resolution helps better capture the subgrid-scale features for the Arctic frontal clouds but does not help improve the simulation of the single-layer boundary layer clouds. This might be because the low resolution climate models could reasonably resolve the single-layer boundary layer clouds, which uniformly covered a large area over NSA and its adjacent oceans during M-PACE. This study indicates that accurate representation of ice crystal number density is important for models to correctly simulate mixed-phase clouds. The parameterizations of ice crystal number density developed based on mid-latitude measurements may not be suitable for use for Arctic clouds.

It has been shown that the model-produced single-layer boundary layer clouds have lower cloud top and cloud base than the observations. This can have a large impact on the surface and TOA radiation. This problem might be related to the low vertical resolution used in these climate models or deficiencies in the model boundary layer parameterizations. A study to examine the impact of increasing model vertical resolution and/or using an improved boundary layer parameterization on the simulated mixed-phase clouds is on-going. We will report the results from this study separately.

Acknowledgments. The work reported here was funded by the US Department of Energy Atmospheric Radiation Measurement Program (ARM) and Climate Change Prediction Program (CCPP). We gratefully thank Drs. G. McFarquhar, D. Turner, Z. Wang, C. Long, and P. Minnis for making the M-PACE field campaign data available for our use. Special thanks go to Dr. R. McCoy for making the aircraft data in a format that can be easily used for model evaluation. We thank Prof. Eugene Clothiaux and Karen Johnson for their help on deriving the cloud fraction from ARSCL products. We thank all the LLNL CAPT team members for their valuable comments on this work. The Climate Data Analysis Tools (CDAT) that were developed in the Program for Climate Model Diagnosis and Intercomparison (PCMDI) were used to perform our analyses. This research was performed under the auspices of the U. S. Department of Energy, Office of Science, Office of Biological and Environmental Research by the University of

California, Lawrence Livermore National Laboratory, under contract W-7405-Eng-48. The Pacific Northwest National Laboratory is operated for the DOE by Battelle Memorial Institute under contract DE-AC06-76RLO 1830.

References

- Bigg, E. K. (1996), Ice forming nuclei in the high Arctic, *Tellus*, 48, 223-233.
- Boyle, J. S. and 8 co-authors (2005), Diagnosis of Community Atmospheric Model 2 (CAM2) in numerical weather forecast configuration at the Atmospheric Radiation Measurement sites, *J. Geophys. Res.*, 110, D15S15, doi:10.1029/2004JD005042.
- Byran, A., P. Rasch, J. Hack, and J. McCaa (2006), Representation of clouds and precipitation processes in the Community Atmosphere Model Version 3 (CAM3), *J. Climate*, 19, 2184 – 2198.
- Clothiaux, E. E., et al. (2000), Objective determination of cloud heights and radar reflectivities using a combination of active remote sensors at the ARM CART sites. *J. Appl. Meteor.*, 39, 645-665.
- Collins, W. D., and co-authors (2006), The formulation and atmospheric simulation of the Community Atmosphere Model Version 3 (CAM3), *J. Climate*, 19, 2144-2161.
- Cotton, W. R., G. J. Tripoli, R. M. Rauber, and E. A. Mulvihill (1986), Numerical simulation of the effects of varying ice crystal nucleation rates and aggregation processes on orographic snowfall, *J. Climate Appl. Meteor.*, 25, 1658–1680.
- Curry, J. A., and Coauthors (2000), FIRE Arctic Clouds Experiment. Overview of Arctic cloud and radiation properties. *Bull. Amer. Meteor. Soc.*, 81, 5-29.
- The GFDL Global Atmospheric Model Development Team (2004), The new GFDL global atmosphere and land model AM2-LM2: Evaluation with prescribed SST simulations, *J. Clim.*, 17, 4641-4673.
- Gregory, D. and D. Morris (1996), The sensitivity of climate simulations to the specification of mixed phase clouds, *Climate Dynamics*, 12, 641-651.
- Hobbs, P. V., and A. L. Rangno (1998), Microstructures of low and middle-level clouds over the Beaufort sea. *Quart. J. Roy. Meteor. Soc.*, 124, 2035-2071.
- Klein, S. A., and C. Jakob (1999), Validation and sensitivities of frontal clouds simulated by the ECMWF model, *Mon. Wea. Rev.*, 127, 2514-2531.
- Li, Z.-X. and H. Le Treut (1992), Cloud-radiation feedbacks in a general circulation model and their dependence on cloud modeling assumptions, *Climate Dyn.*, 7, 133-139.
- Liu, X. and J. E. Penner (2005), Ice nucleation parameterization for global models,

- Meteorologische Zeitschrift* 14, No. 4, 499-514.
- Liu, X. J. E. Penner, S. Ghan, and M. Wang (2007), Inclusion of ice microphysics in the NCAR Community Atmospheric Model version 3 (CAM3), *J. Climate*, in press.
- Lohmann, U. (2002), Possible aerosol effects on ice clouds via contact nucleation, *J. Atmos. Sci.*, **59**, 647–656.
- McFarquhar, G. M., and co-authors (2007), Ice properties of single layer boundary clouds during the Mixed-Phase Arctic Cloud Experiment (MPACE): Part I: Observations, *J. Geophys. Res.*, in press.
- Perovich, D. K., and Coauthors (1999), Year on ice gives climate insights. *Eos, Trans. Amer. Geophys. Union*, **80**, 481.
- Phillips, T. J. and 9 co-authors (2004), Evaluating parameterizations in GCMs: Climate simulation meets weather prediction, *Bull. Am. Meteorol. Soc.*, **85**, 1903-1915.
- Pinto, J. O. (1998), Autumnal mixed-phase cloudy boundary layers in the Arctic, *J. Atmos. Sci.*, **55**, 2016-2038.
- Prezni, A. J. and 8 co-authors (2007), Can ice-nucleating aerosols affect Arctic seasonal climate? Submitted to *Bull. Am. Meteorol. Soc.*
- Rasch, P. J., and J. E. Kristjánsson (1998), A comparison of the CCM3 model climate using diagnosed and predicted condensate parameterizations. *J. Climate*, **11**, 1587-1614.
- Rotstayn, L. D. (1997), A physical based scheme for the treatment of stratiform clouds and precipitation in large-scale models. I: Description and evaluation of the microphysical processes, *Q. J. R. Meteorol. Soc.* **123**, 1227-1282.
- Rotstayn, L. D., B. F. Ryan, and J. J. Katzfey (2000), A scheme for calculation of the liquid fraction in mixed-phase stratiform clouds in large-scale models, *Mon. Weather Rev.*, **128**, 1070-1088.
- Sud, Y. C., D. M. Mocko, and S. J. Lin (2006), Performance of two cloud-radiation parameterization schemes in the finite volume general circulation model for anomalously wet May and June 2003 over the continental United States and Amazonia. *J. Geophys. Res.*, **111**, D06201, doi:10.1029/2005JD006246.
- Tiedtke, M.(1993), Representation of clouds in large-scale models. *Mon. Wea. Rev.*, **121**, 3040-3061.
- Turner, D.D., S.A. Clough, J.C. Liljegren, E.E. Clothiaux, K. Cady-Pereira, and K.L. Gaustad,

- (2007), Retrieving liquid water path and precipitable water vapor from Atmospheric Radiation Measurement (ARM) microwave radiometers. *IEEE Trans. Geosci. Remote Sens.*, *submitted*.
- Uttal, T. et al. (2002), Surface heat budget of the Arctic Ocean. *Bull. Amer. Meteor. Soc.*, **83**, 255-275.
- Verlinde, J. and Coauthors (2007), The Mixed-Phase Arctic Cloud Experiment, *Bull. Am. Meteorol. Soc.*, **88**, 205-221.
- Wang, Z. (2007), Refined two-channel microwave radiometer liquid water path retrieval at cold regions by using multiple-sensor measurements, *submitted to IEEE Geoscience and Remote Sensing Letters*.
- Williamson, D. L., and co-authors (2005), Moisture and temperature balances at the Atmospheric Radiation Measurement Southern Great Plains Site in forecasts with the Community Atmosphere Model (CAM2), *J. Geophys. Res.*, **110**, D15S16, doi:10.1029/2004JD005109.
- Xie, S. M. Zhang, J. S. Boyle, R. T. Cederwall, G. L. Potter, and W. Lin (2004), Impact of a revised convective triggering mechanism on Community Atmosphere Model, Version 2, simulations: Results from short-range weather forecasts, *J. Geophys. Res.*, **109**, D14102, doi:10.1029/2004JD004692.
- Xie, S. C., and Coauthors (2005), Simulations of midlatitude frontal clouds by single-column and cloud-resolving models during the Atmospheric Radiation Measurement March 2000 cloud intensive operational period. *J. Geophys. Res.*, **110**, D15S03, doi:10.1029/2004JD005119.
- Xie, S., S. A. Klein, J. J. Yio, A. C. M. Beljaars, C. N. Long, and M. Zhang (2006), An assessment of ECMWF analyses and model forecasts over the North Slope of Alaska using observations from the ARM Mixed-Phase Arctic Cloud Experiment, *J. Geophys. Res.*, **111**, D05107, doi:10.1029/2005JD006509.
- Zhang, M., W. Lin, C. Bretherton, J. Hack, and P. Rasch (2003), A modified formulation of fractional stratiform condensation rate in the NCAR Community Atmospheric Model (CAM2), *J. Geophys. Res.*, **108**, 4035, doi:10.1029/2002JD002523.
- Zhang, M. H., and Coauthors (2005), Comparing clouds and their seasonal variations in 10 atmospheric general circulation models with satellite measurements, *J. Geophys. Res.*, **110**, D15S01, doi:10.1029/2005JD005923.

Figure Captions

- Figure 1.** Time-height cross sections of cloud fraction (a) ARSCL, (b) CAM3, (c) AM2, and (d) CAM3LIU at Barrow during M-PACE. The unit is %.
- Figure 2.** Time series of the total cloud fraction (%) derived from ARSCL and the models. Black line with dots is for ARSCL, Red line is for CAM3, green for CAMLIU, and blue for AM2.
- Figure 3.** Time-height cross sections of model-produced liquid water mixing ratio (g/kg). (a) CAM3, (b) AM2, and (c) CAM3LIU. The solid lines in the figures are model-simulated temperatures.
- Figure 4.** Same as Figure 3 except for ice water mixing ratio (g/kg).
- Figure 5.** Time series of the observed and model-produced (a) cloud liquid water path (g/m²) and (b) ice water path (g/m²) during M-PACE. The black solid line with dots is from Turner's retrievals and + is from Wang's retrievals. Red lines are for CAM3, green for CAMLIU, and blue for AM2.
- Figure 6.** Liquid fraction as a function of cloud height. (a) UND citation data, (b) CAM3, (c) AM2, and (d) CAM3LIU. Different color dots in (a) represent data collected from different flights. Note that the cloud altitude in the figure is normalized from 0 at cloud base to 1 at cloud top.
- Figure 7.** Liquid fraction as a function of temperature. (a) UND citation data, (b) CAM3, (c) AM2, and (d) CAM3LIU. Different color dots in (a) represent data collected from different flights.
- Figure 8.** Time series of the observed and model-produced (a) surface downwelling longwave radiative fluxes (W/m²) and (b) TOA outgoing longwave radiative fluxes (W/m²). Black lines are observations. Red lines are for CAM3, green for CAMLIU, and blue for AM2.
- Figure 9.** Same as Figure 1 except for (a) AM2N90 and (b) AM2N90N.
- Figure 10.** Same as Figure 5(a) except that red line is for AM2, green for AM2N90, and blue for AM2N90N.

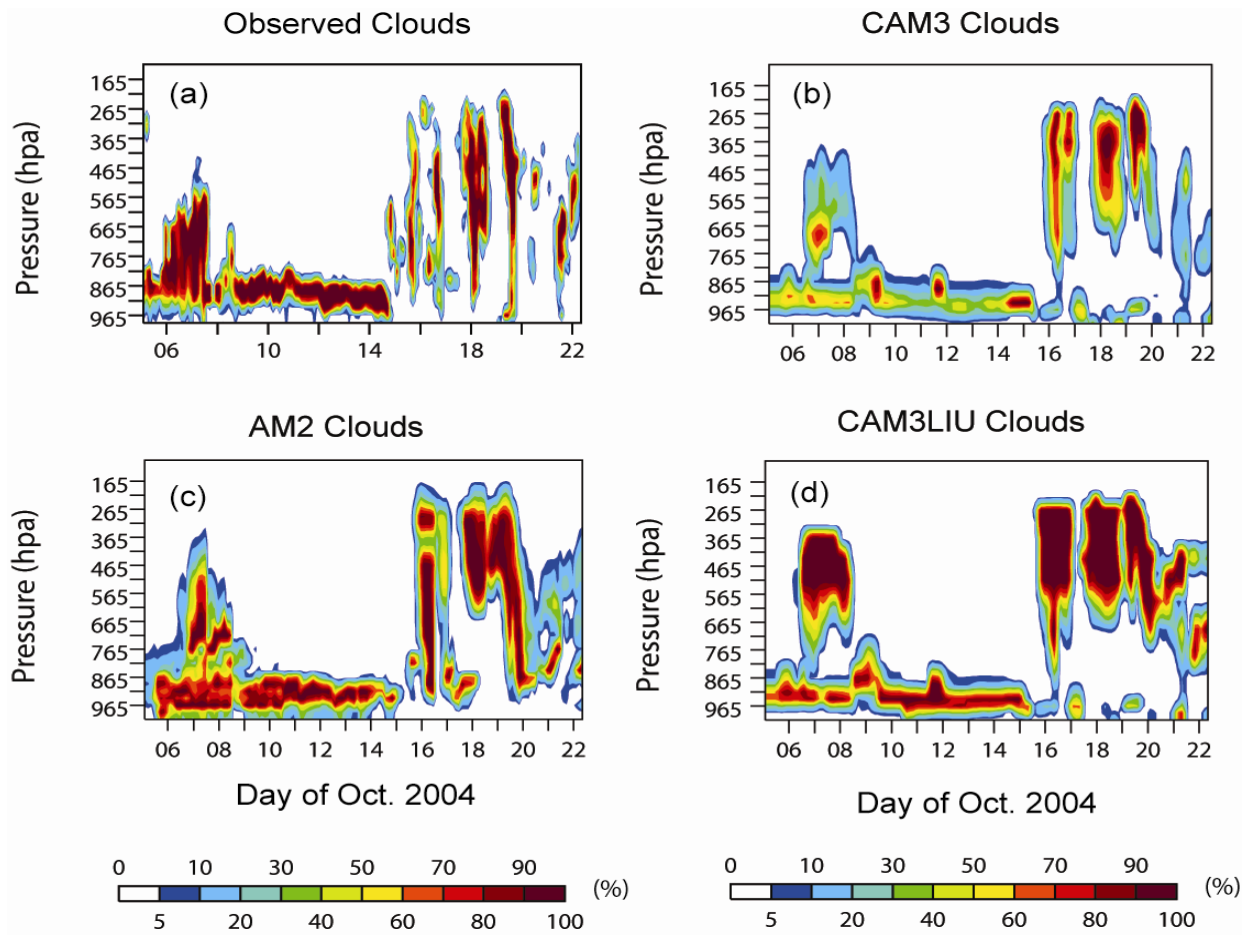


Figure 1. Time-height cross sections of cloud fraction (a) ARSCL, (b) CAM3, (c) AM2, and (d) CAM3LIU at Barrow during M-PACE. The unit is %.

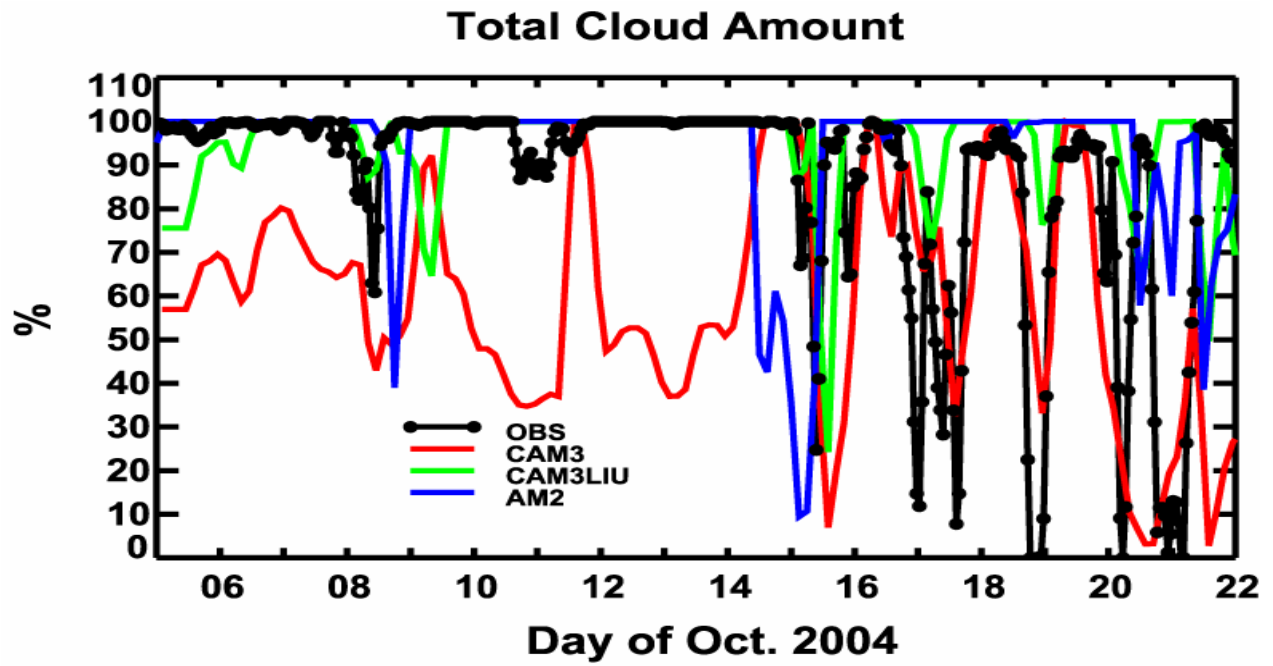


Figure 2. Time series of the total cloud fraction (%) derived from ARSCL and the models. Black line with dots is for ARSCL, Red line is for CAM3, green for CAMLIU, and blue for AM2.

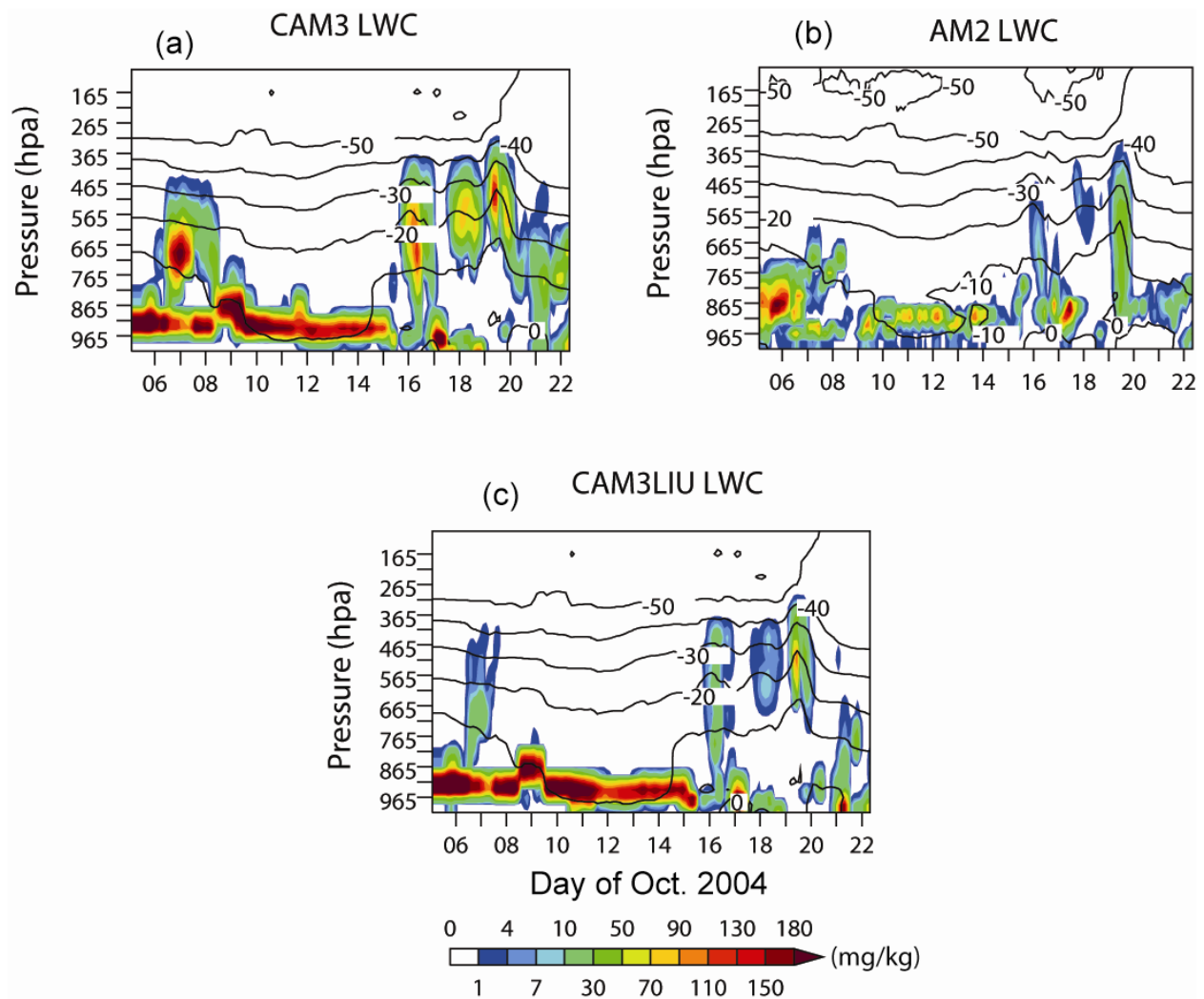


Figure 3. Time-height cross sections of model-produced liquid water mixing ratio (g/kg). (a) CAM3, (b) AM2, and (c) CAM3LIU. The solid lines in the figures are model-simulated temperature.

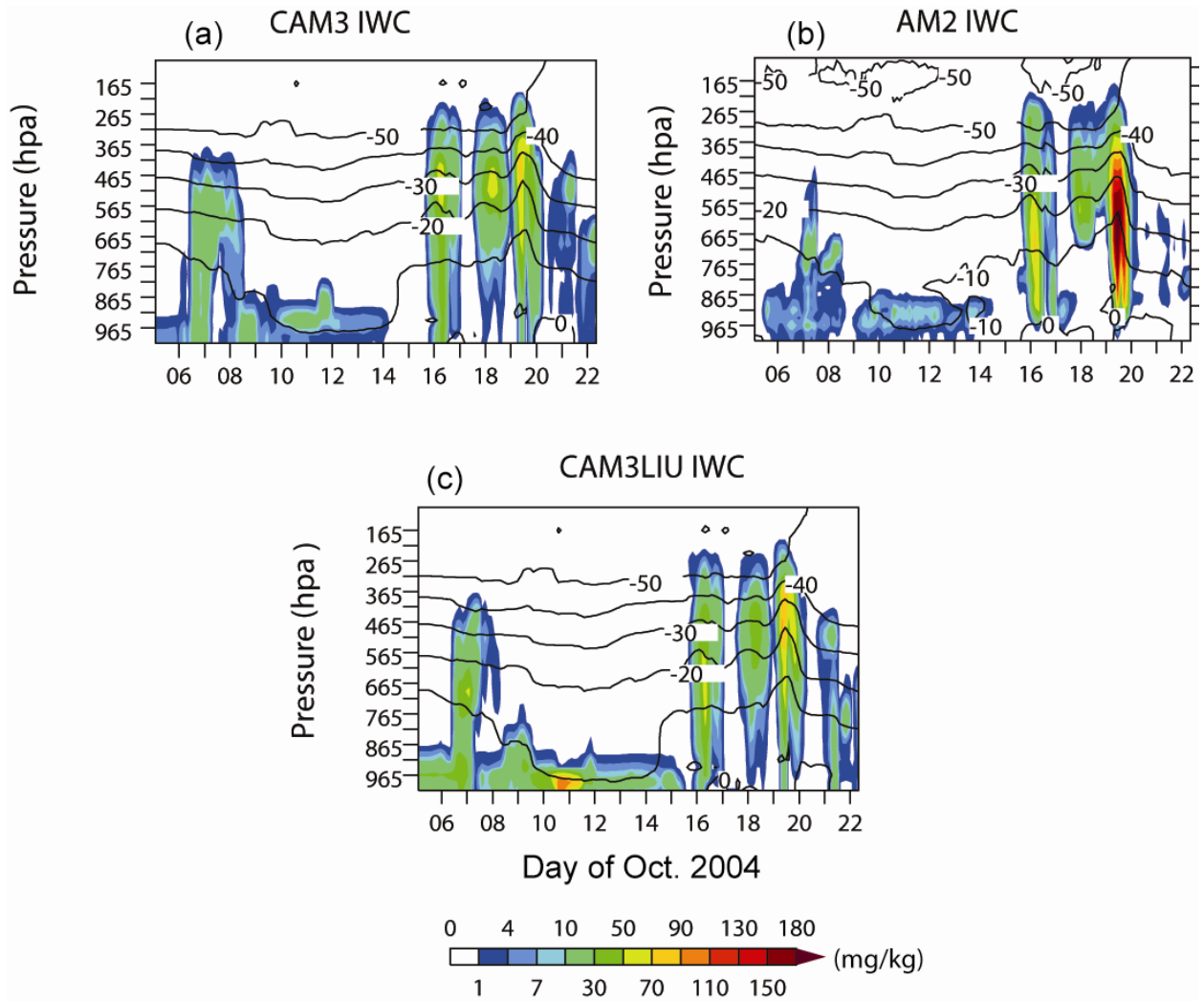


Figure 4. Same as Figure 3 except for ice water mixing ratio (g/kg).

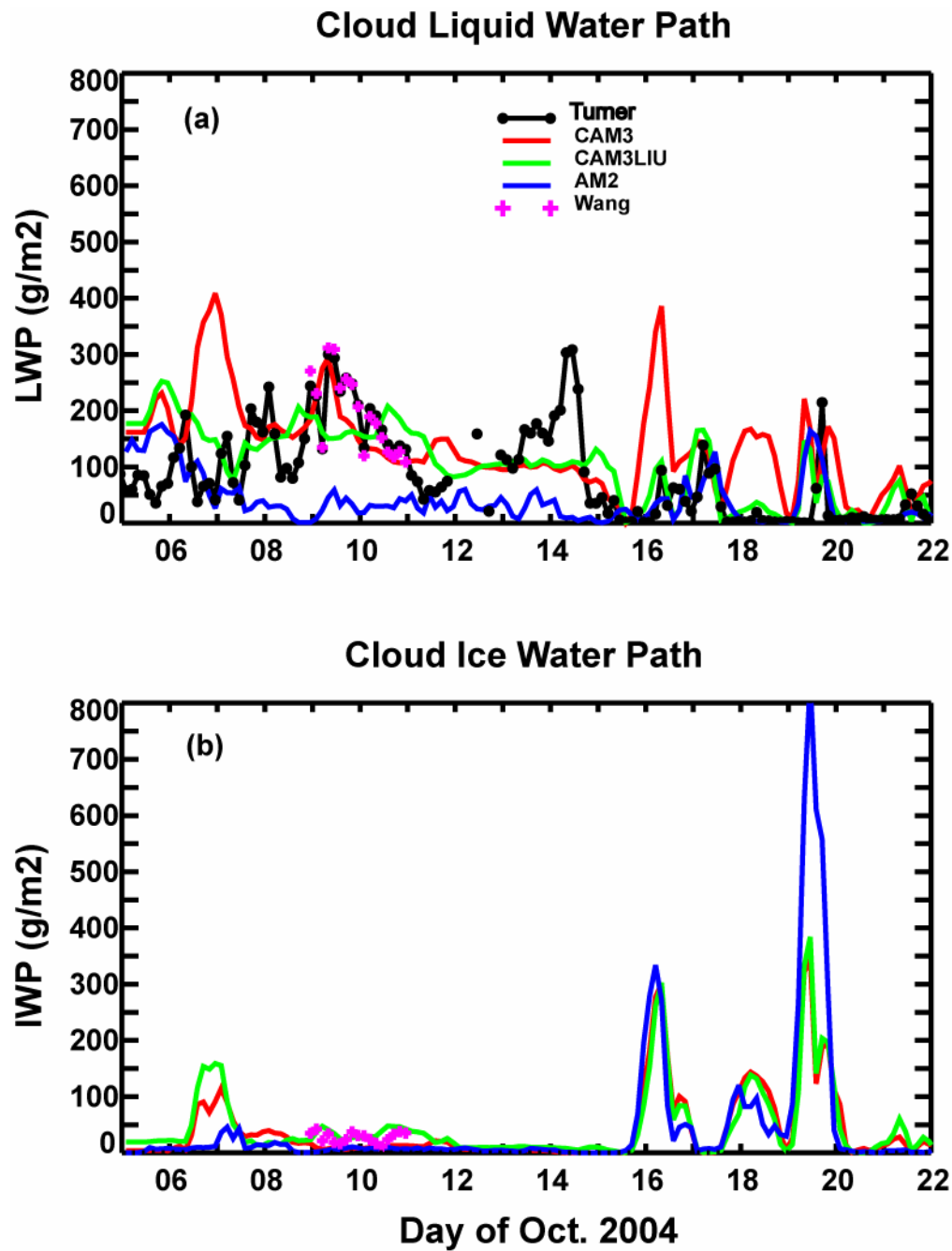


Figure 5. Time series of the observed and model-produced cloud liquid water path (g/m²) and ice water path (g/m²) during M-PACE. Black solid line with dots is from Turner’s retrievals and + is from Wang’s retrievals. Red lines are for CAM3, green for CAMLIU, and blue for AM2.

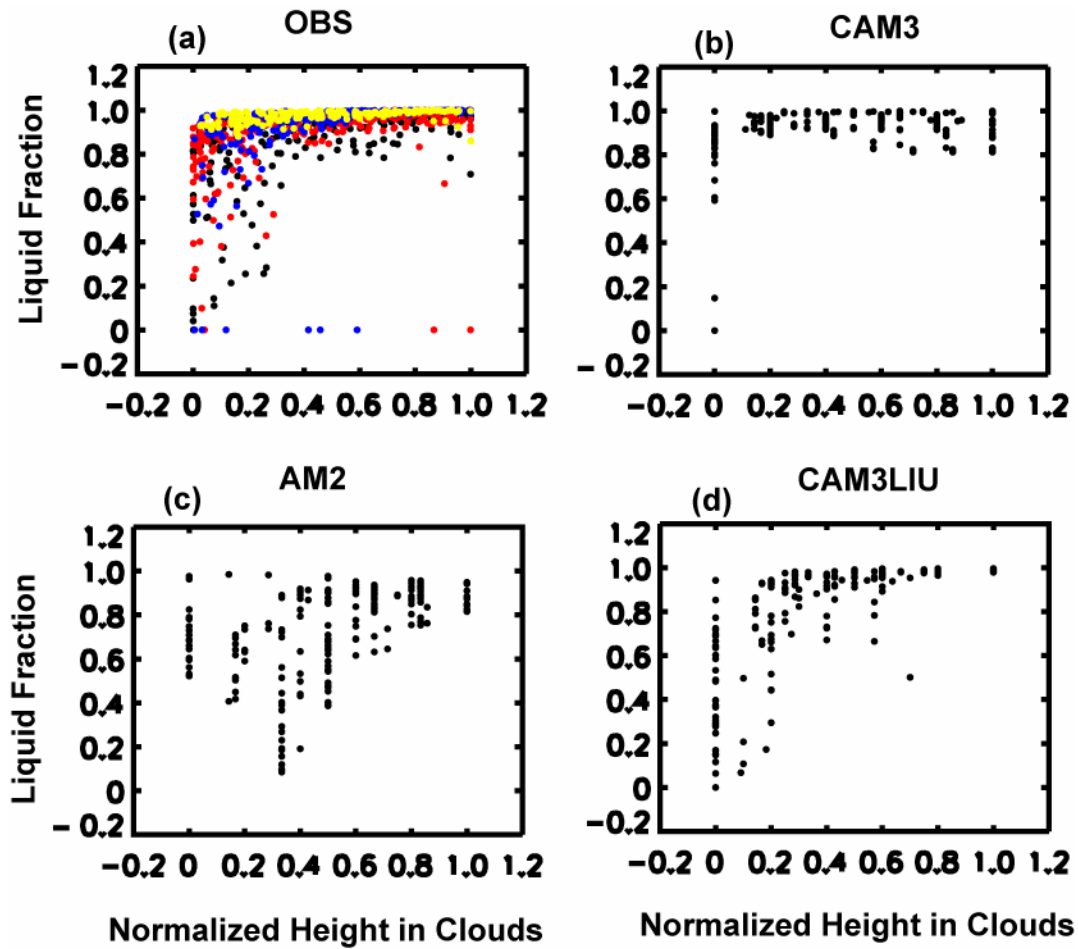


Figure 6. Liquid fraction as a function of cloud height. (a) UND citation data, (b) CAM3, (c) AM2, and (d) CAM3LIU. Different color dots in (a) represent data collected from different flights. Note that the cloud altitude in the figure is normalized from 0 at cloud base to 1 at cloud top.

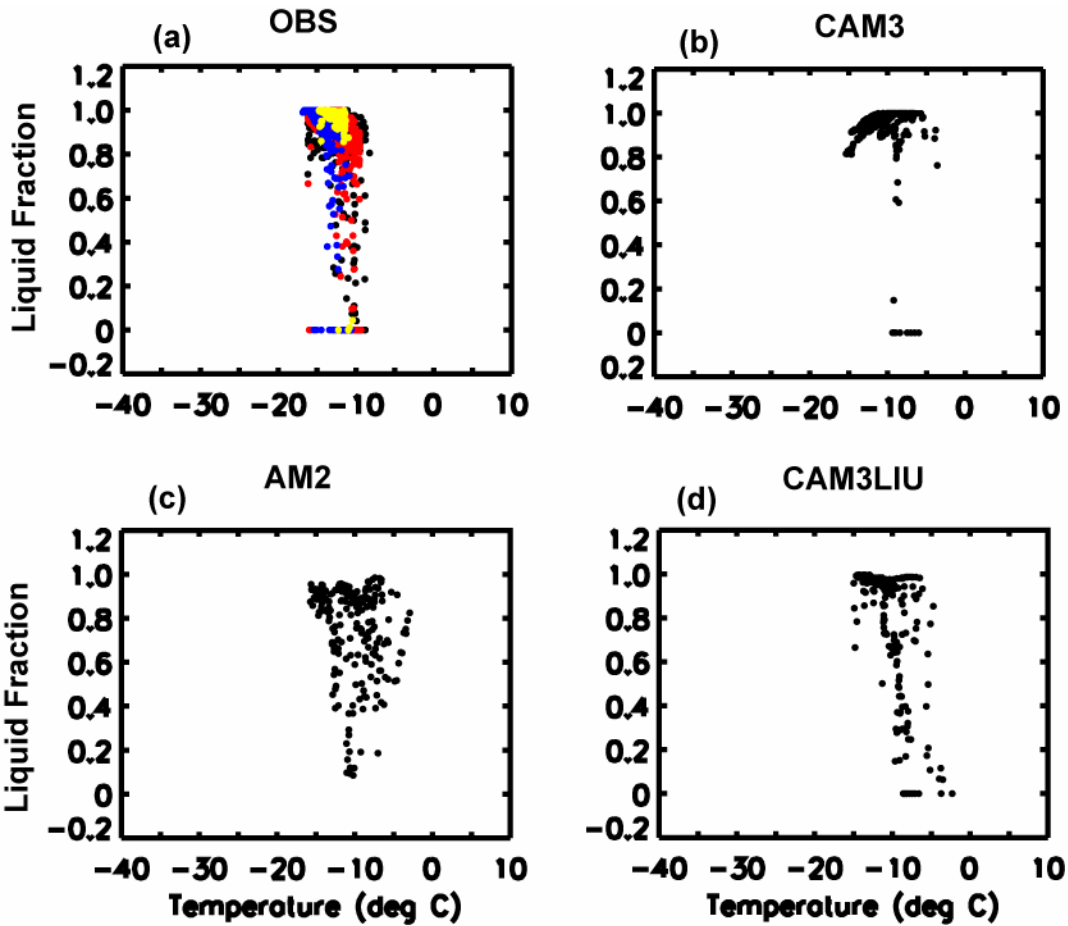


Figure 7. Liquid fraction as a function of temperature. (a) UND citation data, (b) CAM3, (c) AM2, and (d) CAM3LIU. Different color dots in (a) represent data collected from different flights.

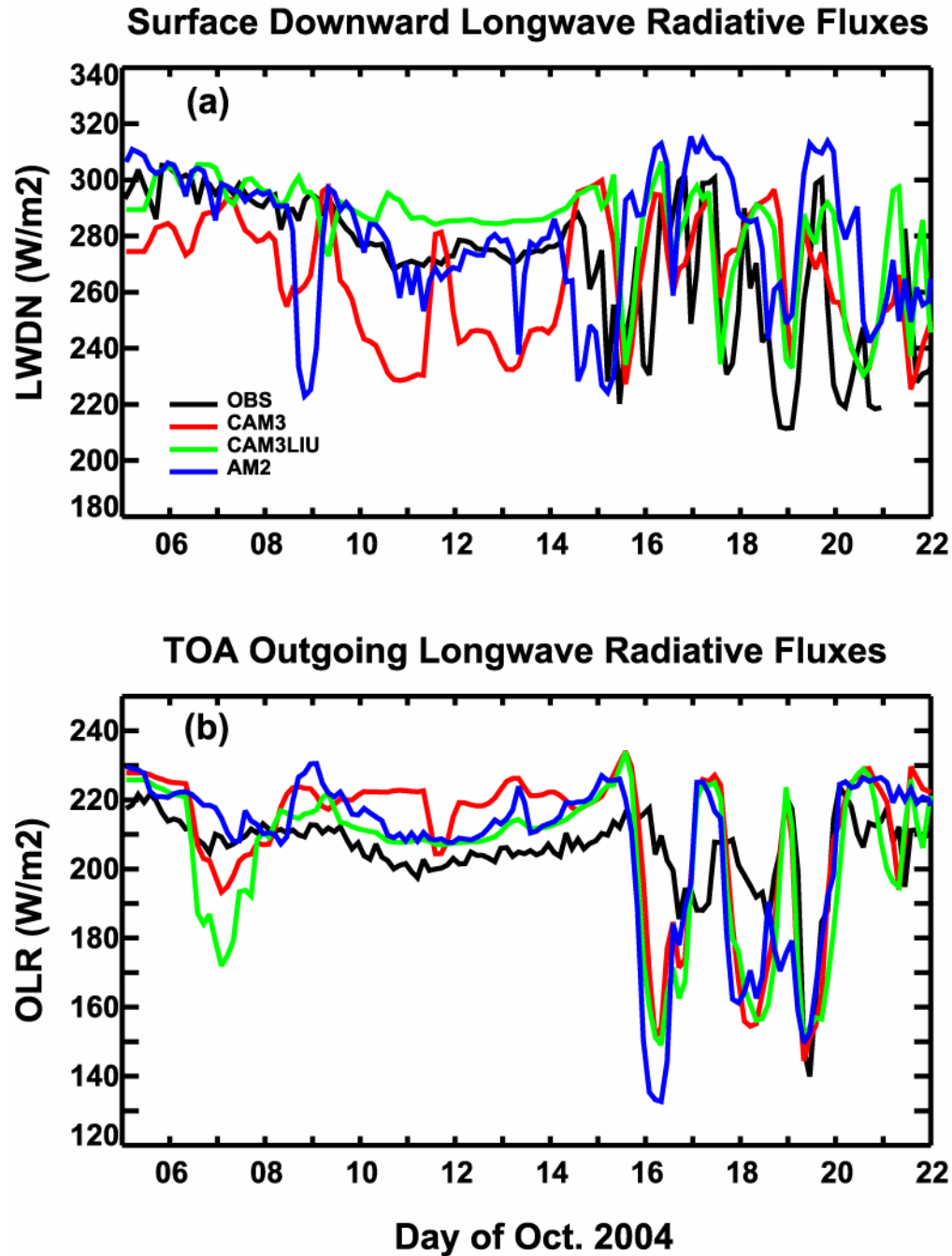


Figure 8. Time series of the observed and model-produced (a) surface downwelling longwave radiative fluxes (W/m²) and (b) TOA outgoing longwave radiative fluxes (W/m²). Black lines are observations. Red lines are for CAM3, green for CAMLIU, and blue for AM2.

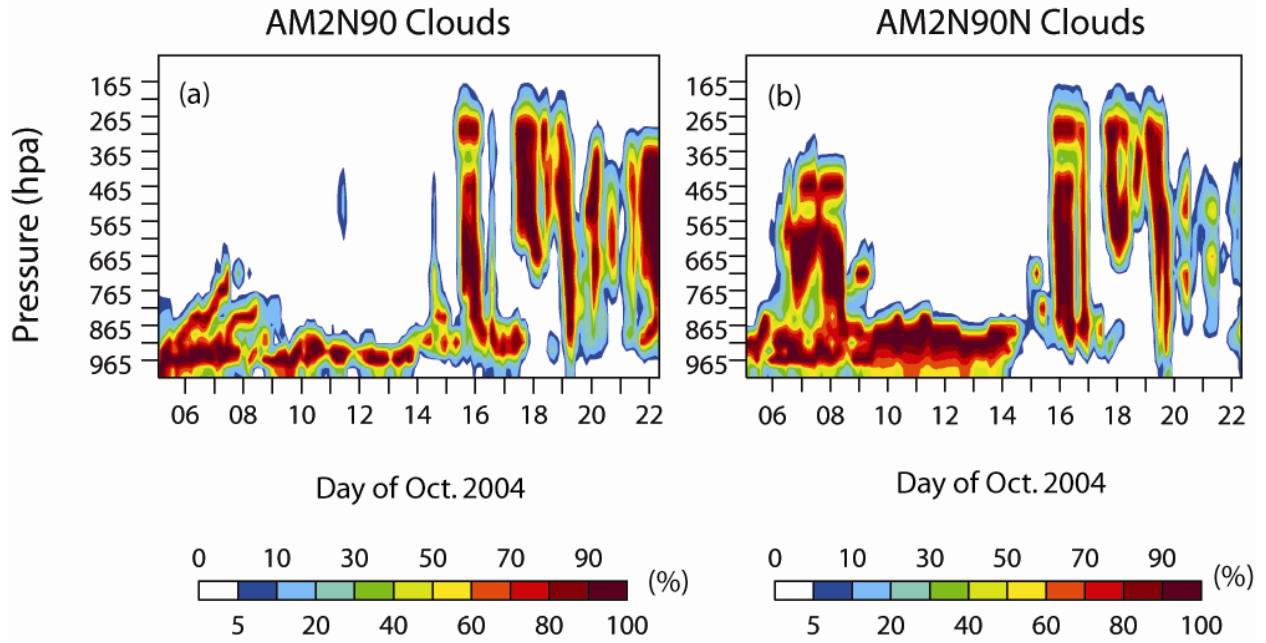


Figure 9. Same as Figure 1 except for (a) AM2N90 and (b) AM2N90N.

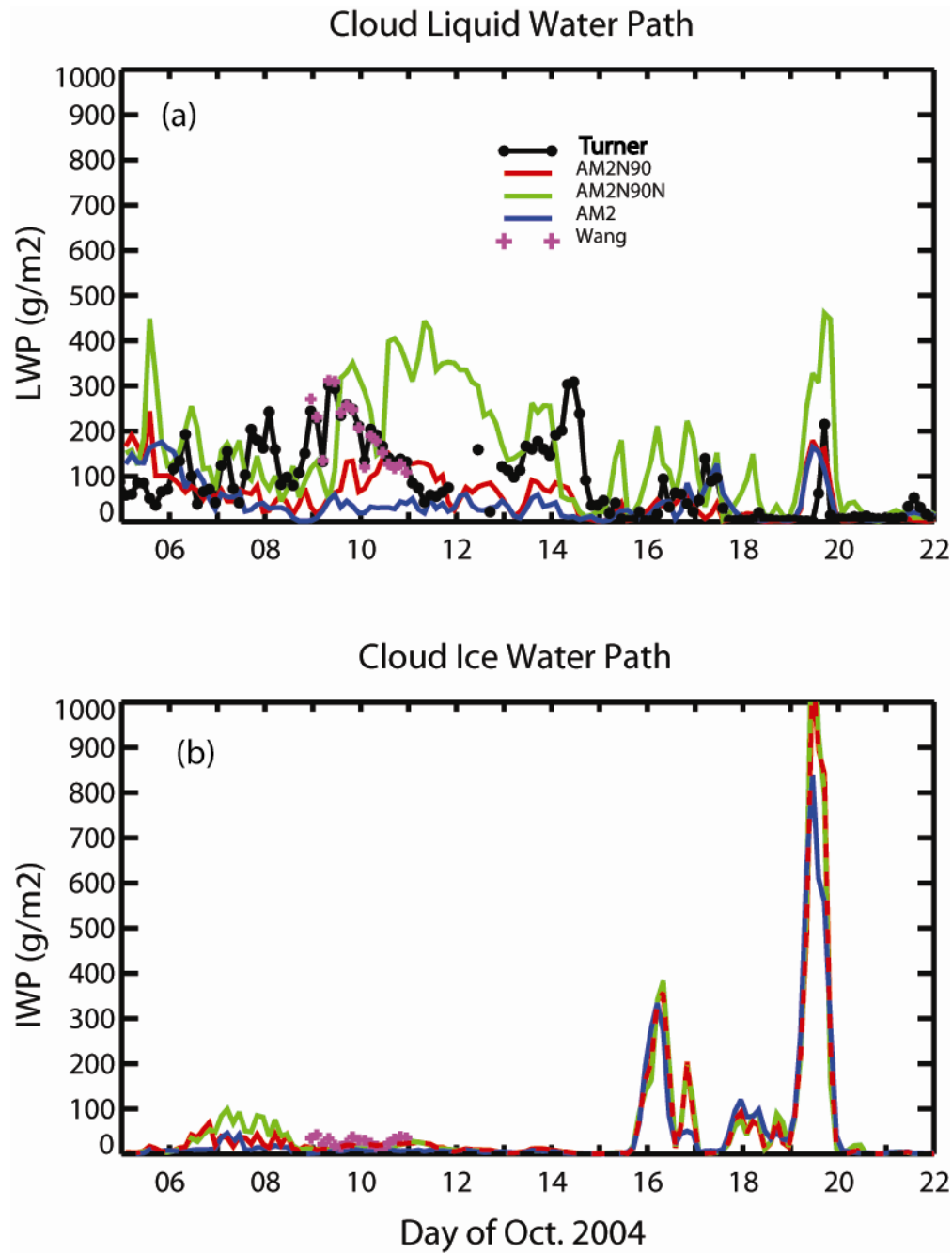


Figure 10. Same as Figure 5(a) except that red line is for AM2, green for AM2N90, and blue for AM2N90N.